Glioblastoma motility occurs in the absence of actin polymer

Andreas Panopoulos[a], Michael Howell[b], Rati Fotedar[a], and Robert L. Margolis[a]
[a]Tumor Development Program, Sanford-Burnham Medical Research Institute, La Jolla, CA 92037; [b]Scripps Research Institute, La Jolla, CA 92037

ABSTRACT **In fibroblasts and keratocytes, motility is actin dependent, while microtubules play a secondary role, providing directional guidance. We demonstrate here that the motility of glioblastoma cells is exceptional, in that it occurs in cells depleted of assembled actin. Cells display persistent motility in the presence of actin inhibitors at concentrations sufficient to fully disassemble actin. Such actin independent motility is characterized by the extension of cell protrusions containing abundant microtubule polymers. Strikingly, glioblastoma cells exhibit no motility in the presence of microtubule inhibitors, at concentrations that disassemble labile microtubule polymers. In accord with an unconventional mode of motility, glioblastoma cells have some unusual requirements for the Rho GTPases. While Rac1 is required for lamellipodial protrusions in fibroblasts, expression of dominant negative Rac1 does not suppress glioblastoma migration. Other GTPase mutants are largely without unique effect, except dominant positive Rac1-Q61L, and rapidly cycling Rac1-F28L, which substantially suppress glioblastoma motility. We conclude that glioblastoma cells display an unprecedented mode of intrinsic motility that can occur in the absence of actin polymer, and that appears to require polymerized microtubules.**

Monitoring Editor
Laurent Blanchoin
CEA Grenoble

Received: Oct 25, 2010
Revised: Apr 4, 2011
Accepted: Apr 22, 2011

INTRODUCTION

Cell motility, as analyzed extensively in mammalian fibroblasts and keratocytes, is an actin-dependent process principally functioning through the extension of lamellipodia or filopodia (Pollard and Borisy, 2003; Rodriguez *et al.*, 2003; Fletcher and Mullins, 2010). In this process the consensus has been that microtubules play a secondary role, guiding directed motility at the leading edge of the cell (Vasiliev *et al.*, 1970; Liao *et al.*, 1995; Nobes and Hall, 1999; Watanabe *et al.*, 2005; Pegtel *et al.*, 2007).

In fibroblasts, dynamic actin fibers drive the formation and extension of leading-edge lamellipodia (Lee *et al.*, 2010). Actin assembly, driven by Arp2/3 production of short dendritic actin networks, is deemed sufficient to change the shape of a cell and produce a protrusion. The polymerization of branched actin filaments at the leading edge is thus believed generally to drive the crawling locomotion of eukaryotic cells (Pollard and Cooper, 2009). In keeping with the central role of actin, the consensus of early literature showed that the actin assembly inhibitor cytochalasin B universally halted cell motility (Wessells *et al.*, 1971). To our knowledge no cell has been observed to migrate in the absence of assembled actin.

We report here that human glioblastoma cells, most remarkably, remain motile in the absence of actin polymers, but their motility ceases when microtubule assembly is suppressed. The motility we observe in the absence of assembled actin involves extension of protrusions toward which the rest of the cell glides. These protrusions have abundant microtubules and no actin fibers, and their morphology is unlike that of lamellipodia or filopodia.

An important aspect of actin-dependent motility is its control by the Rho family GTPases, which cycle between inactive GDP-bound and active GTP-bound states (Hall, 1998). Each of the GTPases characteristically regulates a specific aspect of actin-based motility. Although Rho induces assembly of stress fibers and focal adhesions, Rac induces lamellipodial extensions, and Cdc42 controls filopodial protrusions (Mackay and Hall, 1998). In keeping with their unusual actin-independent motility, migrating glioblastoma cells also have unique requirements for the Rho family GTPases. In primary fibroblasts dominant negative Rac and Cdc42 suppress motility, but we

This article was published online ahead of print in MBoC in Press (http://www.molbiolcell.org/cgi/doi/10.1091/mbc.E10-10-0849) on May 5, 2011.

Address correspondence to: Robert Margolis (rmargolis@sanfordburnham.org).

Abbreviations used: DCB, dihydrocytochalasin B; EGFP, enhanced green fluorescent protein; LatA, latrunculin A; NOC, nocodazole; PI, propidium iodide; TRITC, tetramethyl rhodamine isothiocyanate; VBL, vinblastine.

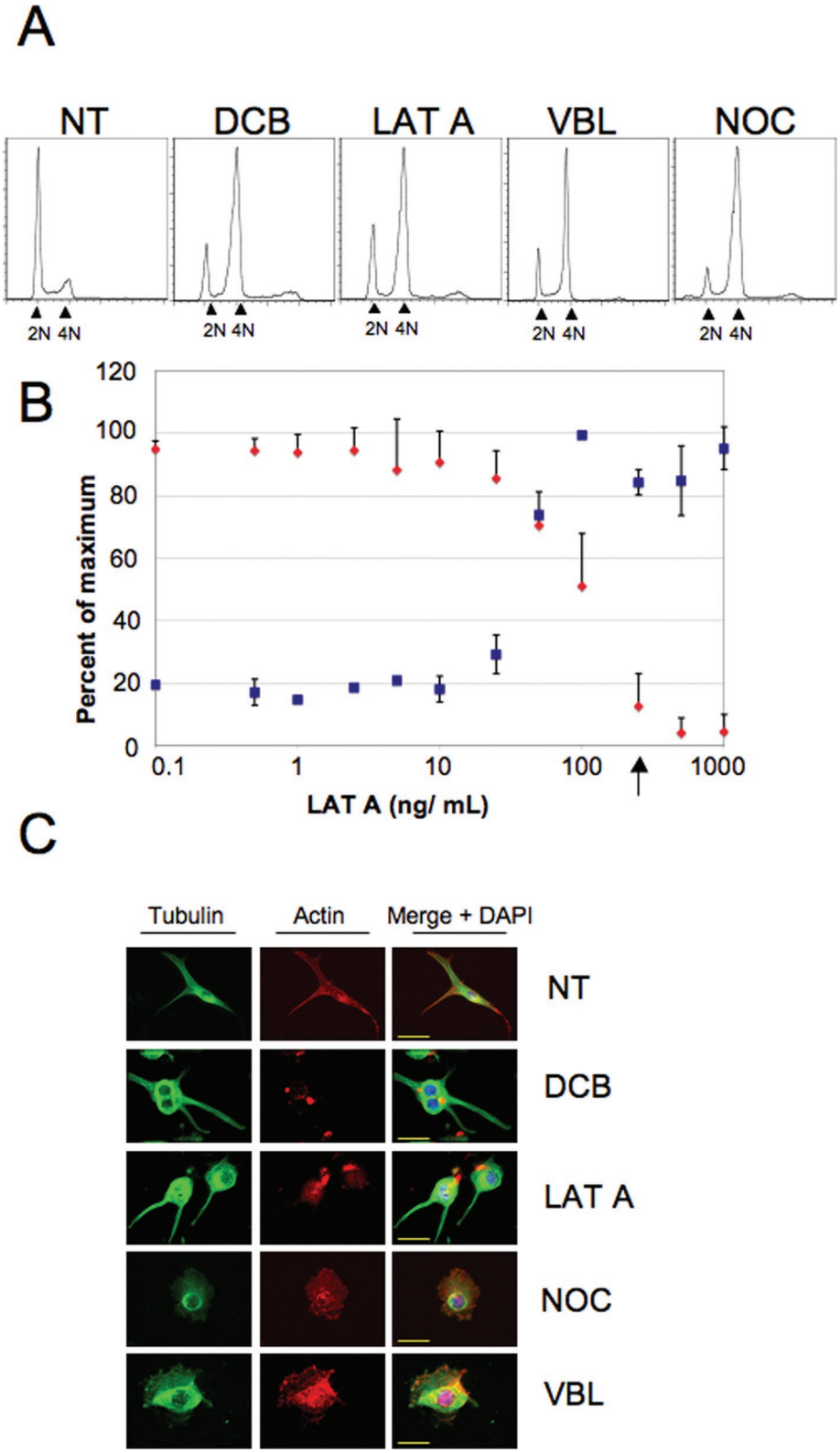

FIGURE 1: Cell cycle and morphological effects of drugs. (A) Flow cytometry profiles of U87MG cells exposed to actin or microtubule inhibitors. U87MG cells were treated with DMSO (NT, not treated), 10 μM DCB, 10 nM VBL, 250 ng/ml of LatA, or 200 ng/ml of NOC for 20 h prior to harvest for fluorescence-activated cell sorting. Unreplicated (2N) and replicated (4N) cell populations are indicated. (B) Quantititative plots of F-actin and DNA content in U87MG cells exposed to varying concentrations of LatA, obtained by flow cytometry. Cells were incubated in the presence or absence of drug for 24 h, then trypsinized and stained with FITC-phalloidin (F-actin) or PI (DNA content). F-actin, red diamonds; DNA content, blue squares. Results are compiled from three independent experiments. Results show that 50 ng/ml of LatA was sufficient to prevent cleavage and 250 ng/ml of LatA effectively suppressed actin assembly. Arrow indicates LatA concentration used in the experiments. (C) Images of U87MG cells exposed to actin and microtubule inhibitors. Cells were exposed to drugs as in A for 24 h and then fixed and stained with anti–α-tubulin (green), TRITC-phalloidin for actin (red), and Hoescht stain for DNA (blue). Note the absence of protrusions with microtubule inhibitors and the presence of protrusions that lack assembled actin (phalloidin binds to assembled actin) with actin inhibitors. All images were acquired using the same exposure times and machine settings for each experimental condition. Scale bar, 7 μm.

find these mutants have almost no effect on glioblastoma cell motility. In contrast, hyperactive Rac1 suppresses motility. These results suggest that glioblastoma cells exhibit a unique motility mechanism. We conclude that glioblastoma cells are capable of migrating in the absence of assembled actin and that they have unusual Rho GTPase requirements.

RESULTS

The roles of actin and microtubules in U87MG motility

In the course of examining cell responses to suppression of actin assembly, we found that U87MG glioblastoma cells exhibited extraordinary motility in the absence of actin fibers but became immotile when microtubule assembly was suppressed.

To determine the relative contributions of the actin and microtubule cytoskeletal networks to glioblastoma motility, we exposed U87MG cells to the actin assembly inhibitors dihydrocytochalasin B (DCB) (10 μM) or latrunculin A (LatA) (250 ng/ml) and to the microtubule assembly inhibitors nocodazole (NOC) (200 ng/ml) or vinblastine (VBL) (100 nM). In our previous work these concentrations were more than sufficient to interfere with the mitotic functions of the respective cytoskeletal networks in a variety of mammalian cells (Lohez *et al.*, 2003). The LatA concentration is more than 10 times the concentration that arrests keratocyte motility (Wilson *et al.*, 2010). We confirmed that exposure of U87MG cells to these drug concentrations for 24 h caused mitotic or cytokinetic failure, yielding cells with 4N DNA content (Figure 1A). These drug concentrations thus suppress either actin or microtubule assembly sufficiently to block cell cycle progression. A titration of LatA showed that cell cleavage was inhibited at 50 ng/ml in U87MG and that actin disassembly appeared nearly complete

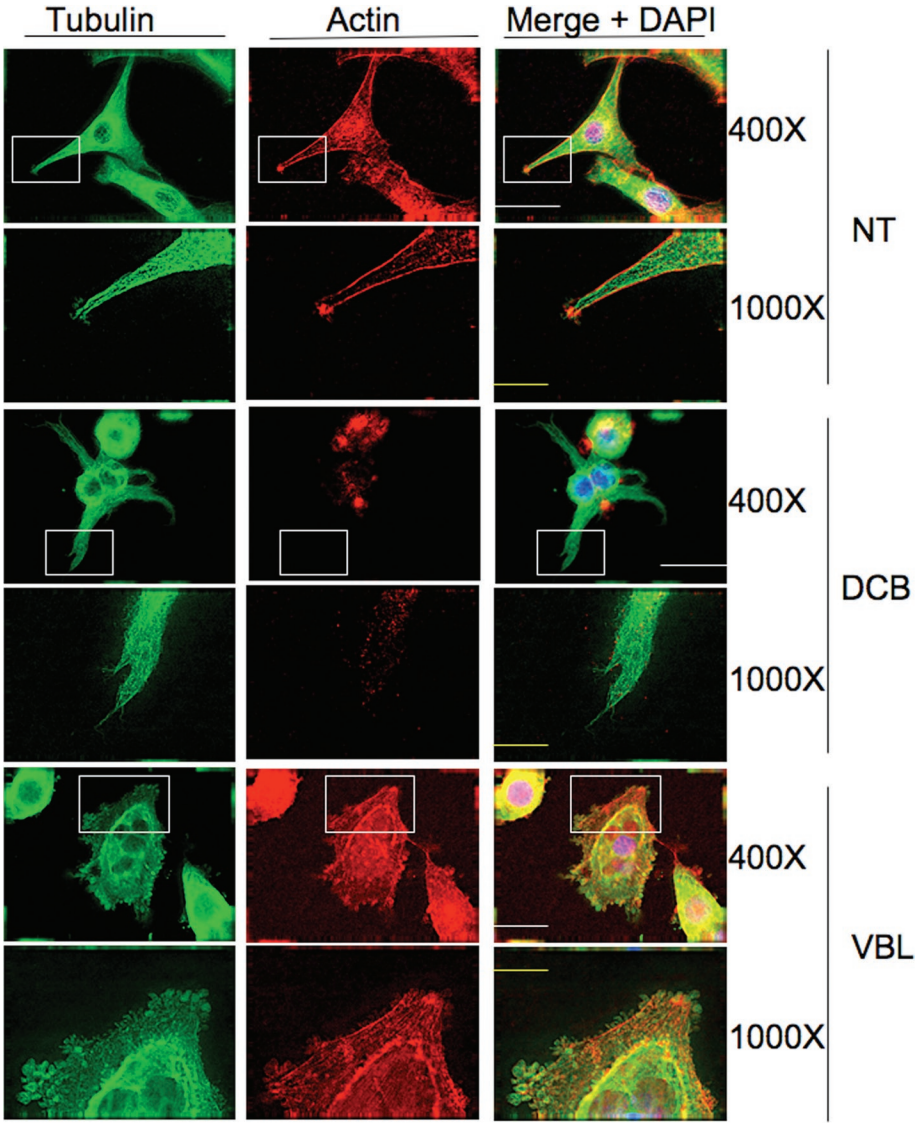

FIGURE 2: High-resolution images of U87MG cells in the presence of actin or microtubule inhibitors. U87MG cells were treated with DMSO (NT), DCB (10 μM), or VBL (100 nM) for 24 h and then fixed and stained with anti–α-tubulin (green), TRITC-phalloidin for actin (red), and Hoescht stain for DNA (blue). Initial images were acquired at 400× magnification to produce a gallery of cells. Then deconvolved 1000× images (boxed areas in the lower-magnification images) were acquired. All images were acquired using the same exposure times and machine settings for each experimental condition. Scale bar at 400×, 7 μm. Scale bar at 1000×, 2 μm.

at 250 ng/ml—the concentration used in our analysis—as determined by flow cytometry quantitation of phalloidin-bound actin (Figure 1B). Similar absence of actin was recorded at 10 μM DCB (unpublished data).

Direct microscopic observation also indicated that suppression of actin assembly was apparently complete in U87MG cells exposed to DCB or to LatA, except for residual punctate foci of actin, whereas the microtubule cytoskeleton appeared intact (Figure 1C). Cell protrusions were abundant in the absence of actin (Figure 2). Cells were binucleate after 24 h, as expected following suppression of cell cleavage. Following either NOC or VBL exposure, actin fibers were abundant (Figure 1) and sometimes were arrayed as stress fibers (Figure 2). There were residual perinuclear microtubules, apparently representing a stable subpopulation. Notably, cells treated with microtubule inhibitors did not extend protrusions.

Following exposure to actin inhibitors, the microtubule arrays within the protrusions, as shown in high-resolution deconvolution microscopy images, appeared well organized and extended to the protrusion leading edge, whereas actin fibers were absent (Figure 2). In contrast, high-resolution images of control cells showed both actin and microtubule fibers throughout the length of cell protrusions. In cells treated with the microtubule inhibitor VBL, actin fibers were abundant, but there were no cell protrusions (Figure 2).

Imaged with time-lapse microscopy, U87MG cells in which actin assembly was suppressed by DCB or LatA demonstrated persistent motility (Supplemental Videos 1 and 2). Cells continuously extended new protrusions and routinely migrated in the direction of one of these protrusions. Periodically, motility would cease, reverse course, or proceed in the direction dictated by another protrusion. At times, some cells rounded up to proceed through mitosis, failed in cleavage, and then reextended protrusions and recommenced migrating (e.g., lower left cell at later times in Supplemental Video 1). The motility observed in control cells is shown for comparison (Supplemental Video 3).

In contrast, U87MG cells exposed to the microtubule inhibitor NOC or VBL rounded up and neither extended protrusions nor migrated. Instead, they consistently oscillated or rotated in place (Supplemental Videos 4 and 5). The motility block was not due to mitotic arrest, as all cells in the population became round, and motility ceased immediately after drug exposure. All of the drug effects on motility in U87MG cells have been replicated with another glioblastoma cell line, C6.

Frames from time-lapse movies show representative fields of cells migrating under different conditions. Colored dots represent the time-dependent change in position of the nuclei of selected cells (Figure 3A). The change with time of the geometric shape linking the marked nuclei documents the displacement of U87 MG cells relative to each other in the presence of DCB but absence of migration on exposure to NOC.

A trajectory representation of the motility of individual U87MG cells relative to the cell position at the *x*- and *y*-axis origin at time zero gives a clear demonstration of the motility of cells under different conditions (Figure 3B). Migration, in the absence of stimulus, appeared to be a persistent random walk (Gail and Boone, 1970). The cells selected for these plots were those closest to the median velocity in several experiments. Migration of cells in the presence of actin inhibitors was similar to that of control cells (Figure 3B, DCB). In contrast, microtubule inhibitors completely suppressed transposition of the selected cells (Figure 3B, NOC). Quantitation of motility from multiple experiments confirms that NOC-treated U87MG cells do not migrate (Figure 4A). Identical results were obtained with VBL

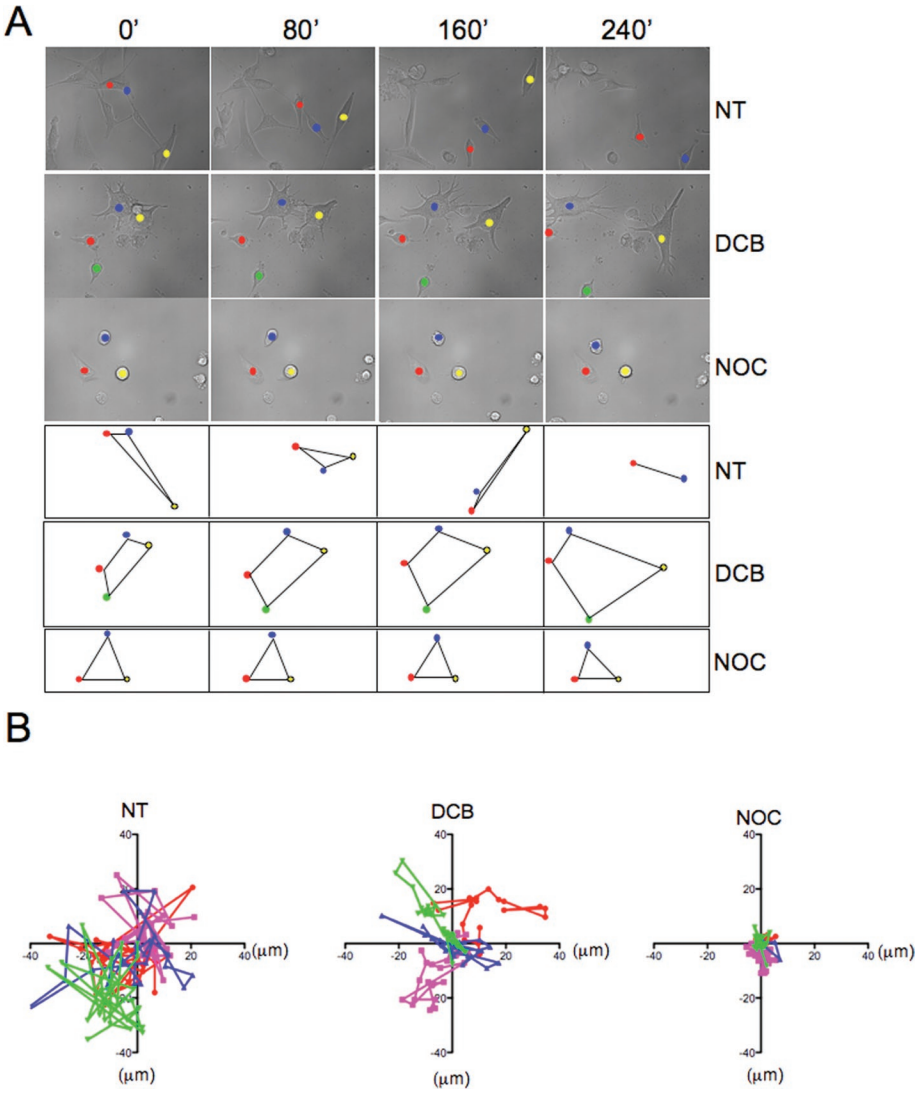

FIGURE 3: Analysis of motility of U87MG cells exposed to actin or microtubule inhibitors. (A) Frames from time-lapse movies. U87MG cells were treated with DMSO (vehicle), DCB (10 μM), or NOC (200 ng/ml) immediately preceding live image acquisition for 24 h at 200× magnification. A series of frames from a 4-h segment is represented. Colored dots (a different color for each tracked cell) were superimposed to easily visualize the motility of selected cells. Below, the colored dots were connected by black lines to visually represent the change in relative cell positions during 6 h. (B) Trajectory representation of cell motility. The trajectories of individual cells were plotted with time for 9 h. Controls and drug exposed cells are as indicated. Point-to-point distances represent change in position at 20-min intervals. The trajectories of control and DCB-treated cells appear to be random walks. No migration occurs in NOC-treated cells. Cells that were closest to median displacement for the indicated treatment were selected from three independent experiments for presentation.

(unpublished data). The cell protrusions in the presence of microtubule inhibitors appeared to be blebs on the basis of rapid-acquisition time-lapse videos (see Supplemental Video 8).

Although actin polymers appear not to be absolutely required for motility of U87MG cells, they appear to enhance the capacity for cell migration. Both the median distance traveled by DCB treated cells and their median velocity are equivalent to the lower quartile median of controls in box and whisker plots of frame-to-frame measurements from videos (Figure 4A). Data (Figure 4A) show that the median distance traveled by controls equals 119.8 μm and velocity equals 0.48 μm/min, whereas DCB median distance equals 81.6 μm and velocity equals 0.27 μm/min. Migration of cells in DCB is characteristically continuous and persistent. An example of the time-dependent motility of the cell perimeter and of the cell centroid of a representative DCB-treated U87MG cell, as resolved using DIAS software, shows consistent motion between video frames (Figure 4B). In contrast, we conducted control time-lapse experiments on primary human foreskin fibroblasts and found, as expected (Wessells *et al.*, 1971), that DCB and LatA, used at the same concentrations as for U87MG, completely blocked motility (unpublished data). Given our finding that actin inhibitors suppress both distance and velocity relative to controls, it is important to note that whereas motility persists in the absence of actin polymer, we cannot rule out that actin polymer, when present, may play a substantial role in U87MG motility.

To assay more directly the role of microtubules in the presence of actin, we assayed the effect of dynein suppression on U87MG cell motility by overexpressing enhanced green fluorescent protein (EGFP)-dynamitin, which effectively suppresses dynein motor function (Etienne-Manneville and Hall, 2001). Dynein, a minus-end-directed microtubule motor, has been reported to regulate the microtubule organizing center (MTOC)–directed polarity of astrocytes (Etienne-Manneville and Hall, 2001). Consistent with a role for microtubules in motility, we found that EGFP-dynamitin had a modest but statistically significant effect on the motility of U87MG cells (Figure 5A). We found a similar effect with expression of the CC1 fragment of p150Glued (unpublished data), also reported to negatively effect dynein-dependent astrocyte MTOC orientation and the direction of cell motility (Etienne-Manneville and Hall, 2001).

The effect of Rho GTPase mutants on motility

Because of their importance to actin-dependent motility, we assayed the effect of the Rho family GTPases RhoA, Rac1, and Cdc42 on U87MG motility. The Rho family of GTPases regulates actin cytoskeletal dynamics by cycling between inactive, GDP-bound and active, GTP-bound states (Hall, 1998) and thus control cell motility in fibroblasts and keratocytes.

Neither native nor dominant negative RhoA (T19N), introduced by transfection as GFP chimeras, had a substantial effect on U87MG motility (Figure 5A), a result significantly variant from the effect of dominant negative RhoA on fibroblast motility (Nobes and Hall, 1999). In addition, dominant negative Rac1 (T17N) was without significant effect on motility (Figure 5A), in contrast to its suppression of directed astrocyte or rat embryo fibroblast motility (Nobes and Hall, 1999). However, we found that dominant negative Cdc42 (T17N) had a modest but significant effect on U87MG motility. In all cases, data were obtained by time-lapse recording of EGFP-positive

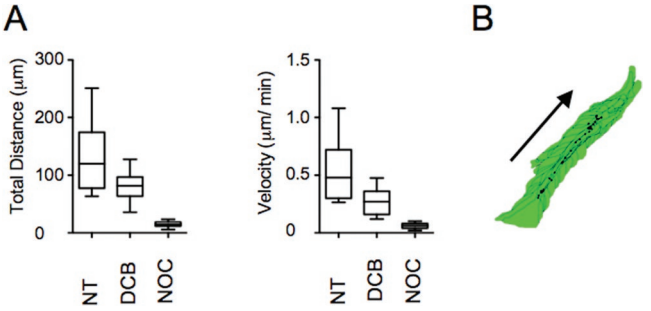

FIGURE 4: Quantitation of motility. (A) U87MG cells were treated with DMSO (NT), DCB (10 µM), or NOC (200 ng/ml) immediately prior to live cell image acquisition. Distances and velocities are the frame-to-frame average from time-lapse recordings, with 20 min elapsed between frames. Fifteen cells per condition were chosen for measurement, and measurements were conducted over a period of 4 h. Only cells that were adherent to the substrate and did not later detach from the chamber slide were counted. Distances and velocities of cells in random fields were measured using softWoRx software as described in *Materials and Methods*. Error bars reflect the standard deviation of measurements in two independent experiments. (B) Displacement of the centroid and cell periphery with time of a cell exposed to DCB, to indicate the consistent velocity of migration along the long axis of the cell. Each dot represents 20-min elapsed time. Image was created from time-lapse video frames with DIAS software.

transfected cells. EGFP-negative cells in the same recordings served as negative controls (Figure 5A, red bars). The data show the percent of the population that is motile. Cells were scored as motile if they persistently moved more than one cell diameter (25 µm) beyond their initial position within the time period of recording. We also scored for relative velocity of cells. Among those cells that were motile in different conditions, there were no significant differences in velocity in time-lapse recordings (unpublished data).

Constitutively active EGFP-Rac1 Q61L completely suppressed the motility of cells either with or without DCB treatment (Figure 5A and Supplemental Video 6). In cells expressing EGFP-Rac1 Q61L, Rac1 overlapped extensively with microtubules in the cell interior but not at the cell periphery (Figure 5B). Stationary DCB-treated Rac1 Q61L–expressing cells rearranged their microtubules into radial arrays, and EGFP-Rac1 Q61L formed aggregates at the cell periphery and in the perinuclear space (Figure 5B). Distinct from cells in the absence of DCB, the Rac1 aggregates did not overlap with microtubules but appeared to be present at points of cell attachment to the substrate (Figure 5B and Supplemental Video 6). This result contrasted with the reported absence of effect of the constitutively active Rac1 Q61L mutant on the motility of fibroblasts (Nobes and Hall, 1999; Pankov *et al.*, 2005) and its enhancement of cell elongation and mesenchymal type motility in melanoma cells (Sanz-Moreno *et al.*, 2008). However, the reported effects of the Q61L mutant occurred under assay conditions different from our two-dimensional random walk. In preliminary experiments, we found that Rac1 Q61L expression partially suppressed normal human fibroblast motility under our conditions.

We considered the possibility that general suppression by constitutively active Rac1 suppressed motility under our conditions because it can interfere with other Rac1 functions that require cycling GTP (Santy, 2002). We therefore also assayed the effect of the spontaneously activated, rapid-cycling, Rac1 F28L mutant (Lin *et al.*, 1999). Although Rac F28L is reported to enhance cortical actin in lamellipodia (Lin *et al.*, 1999), its expression strongly suppressed U87MG motility in the presence or absence of DCB (Figure 5A). Time-lapse video shows Rac F28L–transfected cells that remain stationary while nontransfected cells in the same field migrate from an initial cluster in the presence of DCB (Supplemental Video 7).

We then assayed whether disassembly of microtubules could suppress motility indirectly through effects on Rho GTPases. As noted earlier, NOC treatment blocked motility of U87 cells, and time-lapse video suggested that the cells were blebbing (Supplemental Videos 4 and 5). To confirm this, we performed rapid time-lapse video, which revealed that the surface of NOC-treated cells underwent blebbing rather than ruffling and that the blebbing was suppressed by blebbistatin (Supplementary Video 8), suggesting that Rac1 might not be important to the cell surface phenomena observed in NOC- and VBL-treated cells (Derivery *et al.*, 2008).

We also addressed the possibility that motility might be blocked in NOC- and VBL-treated cells by suppression of RhoA induced by microtubule disassembly. The RhoA suppressor GEF-H1 is sequestered by microtubules, and microtubule disassembly could thus lead to suppression of motility indirectly through RhoGEF-H1 release (Krendel *et al.*, 2002; Chang *et al.*, 2008). If blockage of motility arose from release of RhoGEF-H1 upon microtubule disassembly, expression of a dominant negative RhoGEF-H1 should restore motility in the presence of NOC. We thus expressed GFP-GEF-H1 or dominant negative GEF-H1 Y393A (Krendel *et al.*, 2002) and exposed cells to NOC to address whether microtubules could indirectly affect cell motility through release of RhoGEF-H1. There was no effect of either wild-type GEF-H1 or the GEF-H1 mutant on motility of non–drug-treated cells, and results showed that the mutant was indistinguishable from the wild-type GEF-H1 in failing to rescue motility of NOC-treated cells. As suppression of GEF-H1 does not restore motility in NOC, RhoA hyperactivation through release from disassembled microtubules (Krendel *et al.*, 2002) is not a likely explanation of the failure of U87MG cells to move in NOC. This appears to rule out the possibility that microtubule disassembly suppresses actin-mediated motility through GEF-H1 release.

Both the Rac1 Q61L and F28L mutants suggest that U87MG motility is negatively regulated by hyperactive Rac1. We therefore asked whether loss of microtubules suppressed motility indirectly through hyperactivation of Rac. If this were the case, then the combination of NOC and a dominant negative Rac1 mutant should restore motility. However, cells exposed to the combination of dominant negative Rac1 T17N and NOC were as immotile as cells without Rac1 T17N (Figure 6), ruling out this possibility. This result was consistent with the lack of Rac1-dependent ruffling in NOC-treated cells (Supplemental Video 8). In summary, motility of U87MG cells appears to proceed with little or no Rac1 activity and to be suppressed by constitutively high levels of active Rac1.

DISCUSSION

We have found that motility of human glioblastoma cells proceeds in the absence of intact actin polymers. Suppression of actin assembly with DCB or LatA at concentrations sufficient for complete actin disassembly and more than sufficient to block cell cleavage is permissive for extension of cell protrusions and for sustained motility. In contrast, motility ceases when cells are exposed to the microtubule inhibitors NOC and VBL at minimal concentrations required for mitotic arrest.

To our knowledge, the present work is the first demonstration that interphase cell migration can function independent of actin polymers. These results are clearly divergent from the standard model of cell motility, in which actin-dependent extensions of

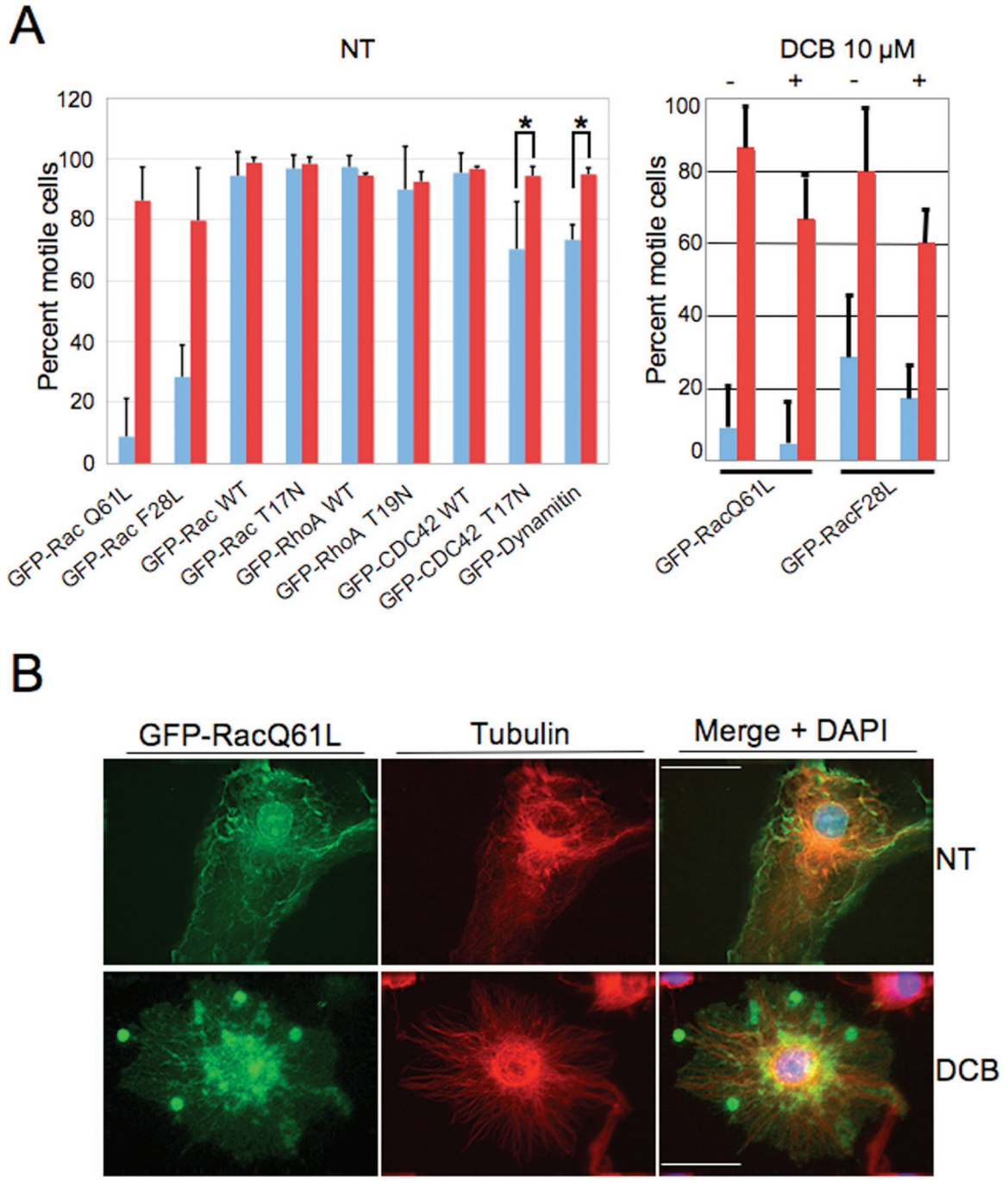

FIGURE 5: Effect of dynein inhibition and of Rac1 mutant expression on motility. The percent motile U87MG cells expressing different Rho GTPase and dynein inhibitor constructs. U87MG cells were transfected with the plasmid constructs indicated. After 24 h, cells were trypsinized and seeded onto eight-chamber glass slides, permitted to adhere for 2 h, then used for live image acquisition for 24 h. Blue bars indicate cells expressing EGFP at levels at least twofold greater than background fluorescence, as quantitated using softWoRx software. Red bars indicate EGFP-negative cells recorded in the same fields (expression of EGFP did not exceed background), which served as controls for motility in the absence of transfection. On the right, cells transfected with EGFP-Rac1 Q61L or Rac1 F28L and exposed to DCB (10 μM) immediately preceding live image acquisition are compared with cells that received EGFP-Rac1 Q61L or Rac1 F28L but no DCB. A minimum of 10 fields per condition were recorded. To quantitate motility, all cells, EGFP positive and negative, were tracked through use of softWoRx software as described in *Materials and Methods*. Error bars reflect standard deviation from two independent experiments. Rac Q61L and Rac F28L are dominant positive, whereas Rac T17N, RhoA T19N, and Cdc42 T17N are dominant negative. WT, wild type.

lamellipodia are the principal means of cell motility, whereas microtubules orient the cell toward a chemotactic gradient (Pollard and Borisy, 2003).

Although microtubules have not been demonstrated previously to move cells independent of actin, previous work has shown that microtubules are important to cell shape changes and to various

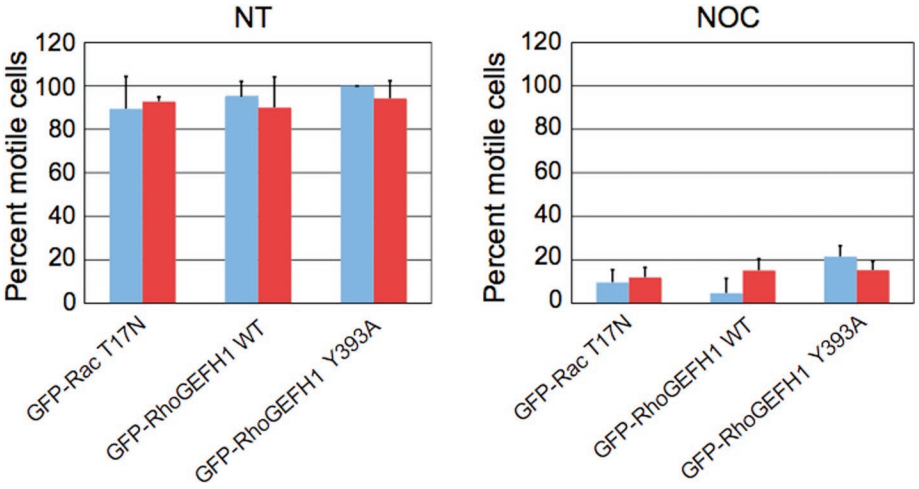

FIGURE 6: Effect of Rac1 T17N and of RhoGEFH1 on motility in NOC. The percent motile U87MG cells expressing different RhoGEFH1 and Rac1 GTPase constructs. U87MG cells were transfected with the plasmid constructs indicated. After 24 h, cells were seeded onto eight-chamber glass slides, permitted to adhere for 2 h, and were then used for live image acquisition for 24 h. Blue bars indicate cells expressing EGFP at levels at least twofold greater than background fluorescence, as quantitated using softWoRx software. Red bars indicate EGFP-negative cells (expression of EGFP did not exceed background) recorded in the same fields, which served as controls for motility in the absence of transfection. Cells transfected with WT RhoGEFH1, dominant negative RhoGEFH1 Y393A. or RacT17N plasmids and exposed to NOC (200 ng/ml) immediately preceding live image acquisition (right) are compared with cells that received the same plasmid transfections but no NOC (left). We recorded a minimum of 10 fields per condition. To quantitate motility, all cells, EGFP positive and negative, were tracked through use of softWoRx software as described in *Materials and Methods*. Error bars reflect standard deviation from two independent experiments. RacT17N and RhoGEFH1 Y393A are dominant negative. WT, wild type.

aspects of cell motility. For example, microtubules generate protrusions in astrocytes (Etienne-Manneville and Hall, 2001) and move the nuclei of neurons following actin-dependent leading-edge migration (Lambert de Rouvroit and Goffinet, 2001; Gerashchenko *et al.*, 2009; Moore *et al.*, 2009). Microtubules are also involved in movement of the cell body toward the lamellipodial leading edge in melanoma cells (Ballestrem *et al.*, 2000), and they have been demonstrated to create cell surface protrusions in MAP2-transfected hepatoma cells following actin disassembly (Edson *et al.*, 1993). Microtubules also are involved in creating cell surface deformations in neural cells and thus are implicated in creating neural extensions (Kaech *et al.*, 1996; Witte *et al.*, 2008). Furthermore, preexisting neurite extensions retract in the presence of microtubule inhibitors (Bray *et al.*, 1978) and have been reported to form in the presence of cytochalasin (Bradke and Dotti, 1999). Thus, microtubules are clearly involved in the motility of intracellular elements in disparate systems. However, the apparent role for microtubules in all aspects of cell motility in glioblastoma in the absence of actin polymer as suggested by our results, is unprecedented. It will be of great interest to determine its mechanism. If microtubules function in this manner, they may do so by interacting with a unique set of proteins. One candidate is the gap junction protein connexin43, a microtubule-anchoring protein (Giepmans *et al.*, 2001) implicated in control of astrocyte motility (Olk *et al.*, 2010). Although it is clear that cells move in an actin-independent manner when exposed to actin assembly inhibitors, it remains to be unequivocally established that glioblastoma cells move in an actin-independent manner when actin polymer is present. Given that Rho GTPase requirements are unusual, we anticipate this may be the case.

The response of U87MG cells to Rho family GTPase dominant mutants also appears to vary substantially from the response of other cell types. In primary fibroblasts dominant negative Rac and Cdc42 suppress motility (Nobes and Hall, 1999). In accord with the unique mode of motility in glioblastoma cells, we found, strikingly, that dominant negative Rac does not affect motility and dominant negative Cdc42 has only a modest effect (Figure 5).

Microtubule disassembly by NOC has been shown to activate RhoA, increasing myosin contractility (Chang *et al.*, 2008) and inducing surface blebbing instead of lamellipodia (Takesono *et al.*, 2010), in part through release of GEF-H1 (Chang *et al.*, 2008). We have observed that NOC induces blebbing, which is reversed by blebbistatin (Supplemental Video 8). However, failure of dominant negative GEF-H1 Y393A to restore motility in NOC-treated cells (Figure 6) suggests that RhoA hyperactivation through release of GEF-H1 from disassembled microtubules (Krendel *et al.*, 2002) is not a likely explanation of the failure of U87MG cells to move in NOC. Furthermore, we found that EGFP-dynamitin, which effectively suppresses dynein motor function (Etienne-Manneville and Hall, 2001), also significantly decreased U87MG motility. These results are consistent with an interpretation that motility is directly dependent on dynamic microtubules even when actin polymer is present. However, other interpretations are possible, and further work is required to resolve this issue.

We found that the constitutively active Rac1 Q61L mutant completely suppresses U87MG motility with or without suppression of actin assembly. However, locking Rac1 in a GTP-bound state can have effects at multiple levels in cells and could thus suppress motility through other mechanisms. We therefore tested the more physiological Rac1 mutant F28L, which is spontaneously activated and rapidly cycling and is capable of transforming cells (Lin *et al.*, 1999). We found the F28L mutant also suppressed motility in U87MG cells. As we have also found a lack of effect of dominant negative Rac1 on U87MG motility, taken together, our results demonstrate that U87MG motility requires little or no Rac1 activity and is actually suppressed by elevated Rac1 activity. Overall, our data are consistent with the lack of a major role for Rho GTPases in glioblastoma motility, with the possible exception of a small but statistically significant effect of Cdc42.

In summary, we have established that complex subcellular systems have the capacity to integrate to enable cell motility in a manner that is independent of assembled actin. Our results further suggest that this motility depends on microtubules. In cells where leading-edge protrusion depends on actin assembly, actin polymerization has been regarded as the motor that converts chemical energy to mechanical energy to drive the cell forward (Theriot, 2000). In the case that microtubules may drive glioblastoma cells forward, one might consider that microtubule dynamics possesses the same capacity for force generation as actin to create motility (Margolis and Wilson, 1981; Inoue and Salmon, 1995; Theriot, 2000).

It is unlikely that such complex actin-independent behavior would have arisen solely in one particular cell type. This opens the question of whether other cells may use an actin-independent motility mechanism similar to that uncovered here. It is further important to note that the actin-independent motility of glioblastoma cells reported here could have implications for tumor therapy, in that it may offer unique targets to suppress aggressive glioblastoma infiltration within the brain parenchyma.

MATERIALS AND METHODS

Equipment and reagents

A Delta Vision Core deconvolution microscope (Applied Precision, Issaquah, WA), equipped with a heated and humidified chamber, was used for all microscopy. LabTek (ThermoFisher Scientific, Waltham, MA) eight-chamber glass slides were used for live cell microscopy. DCB, VBL, and NOC were purchased from EMD Chemicals (San Diego, CA). LatA was purchased from Enzo Life Sciences (Plymouth, PA). pcDNA3-EGFP-Rac1, pcDNA3-EGFP-CDC42, pcDNA3-EGFP-RhoGEFH1, and pcDNA3-EGFP-RhoA wild-type and mutant constructs were kind gifts from the laboratory of Gary Bokoch (Scripps Research Institute, La Jolla, CA) (Zhang *et al.*, 1995). pcDNA3-EGFP-dynamitin (Etienne-Manneville and Hall, 2001) was a kind gift from Trina Schroer (Johns Hopkins University, Baltimore, MD). Mouse monoclonal anti–α-tubulin (B512) and tetramethyl rhodamine isothiocyanate (TRITC)-phalloidin were purchased from Sigma-Aldrich (St. Louis, MO). Lipofectamine 2000, Hoescht 33258 (10 mg/ml), and Alexa Fluor secondary antibodies were purchased from Life Technologies (Carlsbad, CA). Culture media and fetal bovine serum (FBS) were purchased from Mediatech (Manassas, VA).

Cell culture and transfection

U87MG and C6 cells were kind gifts from Carol Kruse and Minoru Fukuda, respectively (both at Sanford-Burnham, La Jolla, CA). U87MG and C6 cells were cultured in DMEM supplemented with 10% FBS and maintained in a humidified incubator at 37°C and 5% CO_2. Transfection of U87MG cells with EGFP-Rho family GTPase or EGFP-dynamitin constructs was done using Lipofectamine 2000 in 12-well plates according to the manufacturer's instructions. At 24 h after transfection, U87MG cells were subjected to time-lapse microscopy for 24 h. Typically, 40% of the cells were EGFP positive, and the EGFP-positive cells were used for quantitative analysis of the effect of the transfected construct on motility. For drug treatment, cells were exposed to the drug concentrations indicated. U87MG cells were exposed to each of the drugs in cultures that were ~50% confluent. Preliminary experiments (unpublished data) confirmed that the concentration of each microtubule inhibitor required to suppress motility was the same as the concentration required to suppress cell division.

Live cell microscopy, cell tracking, and velocity assays

U87MG or C6 cells were seeded at a density of 2×10^4 cells/well in each chamber of a LabTek eight-chamber glass slide. Cells were permitted to settle for 2 h prior to addition of drugs and mounting on the microscope stage. For each experiment, a minimum of 10 fields per chamber at 200× magnification were chosen at random. On average eight cells per field could be observed. Images were taken every 20 min for a period of 24 h using Applied Precision softWoRx software. Stacked image files were then converted to QuickTime or MPEG file formats at 3–5 frames/s. When necessary, the GFP chimera fluorescence intensities were measured with the softWoRx "arbitrary line" tool. To track cell movement, two methods were used: one using softWoRx, the other using DIAS software (Soll Technologies, Iowa City, IA). With the use of softWoRx, points were chosen nearest the center of the nucleus of a cell consecutively for up to 73 frames. By using the "leap frog" tool from softWoRx software, we could measure and record distances traveled and velocity from consecutive frames. Data were then exported to Microsoft Excel to produce plots. The DIAS method used AVI or MPEG files converted from raw Delta Vision files, and whole cells were traced frame by frame. Cell shape and direction were determined using DIAS software.

For rapid time-lapse imaging, U87 cells were exposed to drug (nocodazole or the combination of nocodazole and blebbistatin) for 20 min prior to mounting on the Delta Vision microscope. Images were taken of single cells within a chambered cover glass every 5 s for 20 min. Delta Vision image files were then converted to 14-s QuickTime movies at 17 frames/s.

Immunostaining

For fixed-cell microscopy, U87MG cells were seeded at a density of 1×10^5 cells/well into a 12-well plate preloaded with sterile glass cover slips. Cells were incubated overnight, and drugs were added the next day for 24 h. After drug treatment, cover slips were removed, washed in 1× phosphate-buffered saline (PBS), fixed in 4% formaldehyde, permeabilized, and stained using standard procedures (Skoufias *et al.*, 2007). Primary antibodies (anti–α-tubulin) were used at a 1:500 dilution and incubated for 1 h at 37°C. We used 30 μM TRITC-phalloidin to stain actin fibers. Hoescht 33258 was used to stain nuclei (10 μg/ml).

Flow cytometry

To analyze DNA content, U87MG cells were seeded at 2.5×10^5 cells per well in a six-well plate and incubated 24 h prior to addition of drugs. DCB, NOC, LatA, VBL, or dimethyl sulfoxide (DMSO) (vehicle) was then added to cells for 20 h. After incubation with drugs, cells were trypsinized, washed, and fixed in –20°C methanol for a minimum of 20 min. Fixed samples were then washed once with 1× PBS, stained with a propidium iodide (PI) solution (0.1% Triton X-100, 200 μg/ml of RNAse A, and 20 μg/ml of PI) and analyzed on a Becton Dickinson (San Jose, CA) Excalibur flow cytometer. To analyze F-actin content in cells treated with LatA, cells were trypsinized in the presence of LatA, fixed in 3.7% formaldehyde (for F-actin staining) or –20°C methanol (for DNA content), and stained with fluorescein isothiocyanate (FITC)-phalloidin (Life Technologies, CA) according to the manufacturer's protocol, or with PI. Stained cells were then analyzed by flow cytometry. Nontreated cells served as positive controls for maximum polymerized actin and minimum 4N content, and cells treated with the highest LatA concentrations yielded minimum polymerized actin and maximum 4N content. With the use of FloJo software (Ashland, OR) a gate was created to sort F-actin–positive cells from negative cells and quantitate the F-actin signal. The resulting histograms were plotted in Excel as percent of maximum versus concentration of LatA.

ACKNOWLEDGMENTS

We thank Trina Schroer (Johns Hopkins University) and the laboratory of Gary Bokoch (Scripps Research Institute) for generously supplying plasmids and Carol Kruse and Minoru Fukuda (Sanford-Burnham) for cell lines. This work was supported by NIH Grants RO1GM068107 and RO1GM088716 (R.L.M.) and RO1CA101810 (R.F.).

REFERENCES

Ballestrem C, Wehrle-Haller B, Hinz B, Imhof BA (2000). Actin-dependent lamellipodia formation and microtubule-dependent tail retraction control-directed cell migration. Mol Biol Cell 11, 2999–3012.

Bradke F, Dotti CG (1999). The role of local actin instability in axon formation. Science 283, 1931–1934.

Bray D, Thomas C, Shaw G (1978). Growth cone formation in cultures of sensory neurons. Proc Natl Acad Sci USA 75, 5226–5229.

Chang YC, Nalbant P, Birkenfeld J, Chang ZF, Bokoch GM (2008). GEF-H1 couples nocodazole-induced microtubule disassembly to cell contractility via RhoA. Mol Biol Cell 19, 2147–2153.

Derivery E, Fink J, Martin D, Houdusse A, Piel M, Stradal TE, Louvard D, Gautreau A. (2008). Free Brick1 is a trimeric precursor in the assembly of a functional wave complex. PLoS One 3, e2462.

Edson K, Weisshaar B, Matus A (1993). Actin depolymerisation induces process formation on MAP2-transfected non-neuronal cells. Development 117, 689–700.

Etienne-Manneville S, Hall A (2001). Integrin-mediated activation of Cdc42 controls cell polarity in migrating astrocytes through PKCzeta. Cell 106, 489–498.

Fletcher DA, Mullins RD (2010). Cell mechanics and the cytoskeleton. Nature 463, 485–492.

Gail MH, Boone CW (1970). The locomotion of mouse fibroblasts in tissue culture. Biophys J 10, 980–993.

Gerashchenko MV, Chernoivanenko IS, Moldaver MV, Minin AA (2009). Dynein is a motor for nuclear rotation while vimentin IFs is a "brake." Cell Biol Int 33, 1057–1064.

Giepmans BN, Verlaan I, Hengeveld T, Janssen H, Calafat J, Falk MM, Moolenaar WH (2001). Gap junction protein connexin-43 interacts directly with microtubules. Curr Biol 11, 1364–1368.

Hall A (1998). Rho GTPases and the actin cytoskeleton. Science 279, 509–514.

Inoue S, Salmon ED (1995). Force generation by microtubule assembly/disassembly in mitosis and related movements. Mol Biol Cell 6, 1619–1640.

Kaech S, Ludin B, Matus A (1996). Cytoskeletal plasticity in cells expressing neuronal microtubule-associated proteins. Neuron 17, 1189–1199.

Krendel M, Zenke FT, Bokoch GM (2002). Nucleotide exchange factor GEF-H1 mediates cross-talk between microtubules and the actin cytoskeleton. Nat Cell Biol 4, 294–301.

Lambert de Rouvroit C, Goffinet AM (2001). Neuronal migration. Mech Dev 105, 47–56.

Lee CS, Choi CK, Shin EY, Schwartz MA, Kim EG (2010). Myosin II directly binds and inhibits Dbl family guanine nucleotide exchange factors: a possible link to Rho family GTPases. J Cell Biol 190, 663–674.

Liao G, Nagasaki T, Gundersen GG (1995). Low concentrations of nocodazole interfere with fibroblast locomotion without significantly affecting microtubule level: implications for the role of dynamic microtubules in cell locomotion. J Cell Sci 108, (Pt 11), 3473–3483.

Lin R, Cerione RA, Manor D (1999). Specific contributions of the small GTPases Rho, Rac, and Cdc42 to Dbl transformation. J Biol Chem 274, 23633–23641.

Lohez OD, Reynaud C, Borel F, Andreassen PR, Margolis RL (2003). Arrest of mammalian fibroblasts in G1 in response to actin inhibition is dependent on retinoblastoma pocket proteins but not on p53. J Cell Biol 161, 67–77.

Mackay DJ, Hall A (1998). Rho GTPases. J Biol Chem 273, 20685–20688.

Margolis RL, Wilson L (1981). Microtubule treadmills–possible molecular machinery. Nature 293, 705–711.

Moore JK, Sept D, Cooper JA (2009). Neurodegeneration mutations in dynactin impair dynein-dependent nuclear migration. Proc Natl Acad Sci USA 106, 5147–5152.

Nobes CD, Hall A (1999). Rho GTPases control polarity, protrusion, and adhesion during cell movement. J Cell Biol 144, 1235–1244.

Olk S, Turchinovich A, Grzendowski M, Stuhler K, Meyer HE, Zoidl G, Dermietzel R (2010). Proteomic analysis of astroglial connexin43 silencing uncovers a cytoskeletal platform involved in process formation and migration. Glia 58, 494–505.

Pankov R, Endo Y, Even-Ram S, Araki M, Clark K, Cukierman E, Matsumoto K, Yamada KM (2005). A Rac switch regulates random versus directionally persistent cell migration. J Cell Biol 170, 793–802.

Pegtel DM, Ellenbroek SI, Mertens AE, Van Der Kammen RA, de Rooij J, Collard JG (2007). The Par-Tiam1 complex controls persistent migration by stabilizing microtubule-dependent front-rear polarity. Curr Biol 17, 1623–1634.

Pollard TD, Borisy GG (2003). Cellular motility driven by assembly and disassembly of actin filaments. Cell 112, 453–465.

Pollard TD, Cooper JA (2009). Actin, a central player in cell shape and movement. Science 326, 1208–1212.

Rodriguez OC, Schaefer AW, Mandato CA, Forscher P, Bement WM, Waterman-Storer CM (2003). Conserved microtubule-actin interactions in cell movement and morphogenesis. Nat Cell Biol 5, 599–609.

Santy LC (2002). Characterization of a fast cycling ADP-ribosylation factor 6 mutant. J Biol Chem 277, 40185–40188.

Sanz-Moreno V, Gadea G, Ahn J, Paterson H, Marra P, Pinner S, Sahai E, Marshall CJ (2008). Rac activation and inactivation control plasticity of tumor cell movement. Cell 135, 510–523.

Skoufias DA, Indorato RL, Lacroix F, Panopoulos A, Margolis RL (2007). Mitosis persists in the absence of Cdk1 activity when proteolysis or protein phosphatase activity is suppressed. J Cell Biol 179, 671–685.

Takesono A, Heasman SJ, Wojciak-Stothard B, Garg R, Ridley AJ (2010). Microtubules regulate migratory polarity through Rho/ROCK signaling in T cells. PLoS One 5, e8774.

Theriot JA (2000). The polymerization motor. Traffic 1, 19–28.

Vasiliev JM, Gelfand IM, Domnina LV, Ivanova OY, Komm SG, Olshevskaja LV (1970). Effect of colcemid on the locomotory behaviour of fibroblasts. J Embryol Exp Morphol 24, 625–640.

Watanabe T, Noritake J, Kaibuchi K (2005). Regulation of microtubules in cell migration. Trends Cell Biol 15, 76–83.

Wessells NK, Spooner BS, Ash JF, Bradley MO, Luduena MA, Taylor EL, Wrenn JT, Yamaa K (1971). Microfilaments in cellular and developmental processes. Science 171, 135–143.

Wilson CA, Tsuchida MA, Allen GM, Barnhart EL, Applegate KT, Yam PT, Ji L, Keren K, Danuser G, Theriot JA (2010). Myosin II contributes to cell-scale actin network treadmilling through network disassembly. Nature 465, 373–377.

Witte H, Neukirchen D, Bradke F (2008). Microtubule stabilization specifies initial neuronal polarization. J Cell Biol 180, 619–632.

Zhang S, Han J, Sells MA, Chernoff J, Knaus UG, Ulevitch RJ, Bokoch GM (1995). Rho family GTPases regulate p38 mitogen-activated protein kinase through the downstream mediator Pak1. J Biol Chem 270, 23934–23936.